Advances in Applied Mathematics and Mechanics
Adv. Appl. Math. Mech., Vol. **8**, No. 5, pp. 827-846

DOI: 10.4208/aamm.2015.m1001
October 2016

Modeling and Computation of CO_2 Allowance Derivatives Under Jump-Diffusion Processes

Shuhua Zhang[1,2,*] and Jing Wang[3,1]

[1] *Research Center for Mathematics and Economics, Tianjin University of Finance and Economics, Tianjin 300222, China*
[2] *Institute of Policy and Management, Chinese Academy of Sciences, Beijing 100190, China*
[3] *Department of Mathematics and Physics, Bengbu College, Bengbu, 233030, China*

Received 10 March 2015; Accepted (in revised version) 18 August 2015

Abstract. In this paper, we study carbon emission trading whose market is gaining in popularity as a policy instrument for global climate change. The mathematical model is presented for pricing options on CO_2 emission allowance futures with jump diffusion processes, and a so-called fitted finite volume method is proposed to solve the pricing model for the spatial discretization, in which the Crank-Nicolson is employed for time stepping. In addition, the stability and the convergence of the fully discrete scheme are given, and some numerical results, which are compared with the closed form solution and the Monte Carlo simulation solution, are provided to demonstrate the rates of convergence and the robustness of the numerical method.

AMS subject classifications: 65M12, 65M60, 91B28

Key words: CO_2 emission allowance, option pricing, jump diffusion, fitted finite volume method, partial integro-differential equation, fast Fourier transform.

1 Introduction

Global climate warming and its dangerous ecological, social, and economic consequences have gained increasing public attention in recent years. The increasing concentration of greenhouse gases (GHGs) in the atmosphere over the past century is to some extent related to human activities, among which, first of all, the emitted CO_2 characterized by an essential increase in human fossil fuel consumption is. Now carbon emission allowance trading has been accepted as a way to reduce emissions at the lowest abatement cost by adding economic cost to carbon emissions, which is an environmental policy device.

*Corresponding author.
Email: shuhua55@126.com (S. H. Zhang), crysralstella@126.com (J. Wang)

 ©2016 Global Science Press

https://doi.org/10.4208/aamm.2015.m1001 Published online by Cambridge University Press

Up to now, emission trading schemes have been designed by introducing appropriate market mechanisms. For example, the European Union emission trading scheme (EU ETS), a cap and trade system, is the most prominent example. Within this scheme, each member state receives a fixed amount of EUA (European Union Allowance), which is called the cap. The European Union started with a pilot period, 2005-2007, followed by the Kyoto commitment period 2008-2012. The third period will last from 2013 to 2020.

Also, the same efforts are being made in China. In fact, the emissions trading platforms have opened in China in the cities/provinces undertaking pilot stage GHG mitigation, which are exclusive and are not yet linked. They will be linked within the nationwide emissions trading system after 2015 or 2016. China's trading programs are now becoming the second largest emissions trading scheme following the EU ETS. Before the emissions trading platforms opened, China had already experienced with the carbon market through the CERs (Certified Emissions Reduced) produced by the Clean Development Mechanism (CDM) projects under the Kyoto Protocol. In addition, in October of 2011, the National Development Reform Commission (NDRC) designated seven provinces and cities, Guangdong, Hubei, Beijing, Shanghai, Tianjin, Chongqing, and Shenzhen, as regional mandatory ETS pilots (see Fig. 1). Most of the pilot regions should submit their ETS implementation plans to the NDRC. A national ETS is also under consideration.

Similar to all other financial or commodity markets, both regulated companies and investors are subject to carbon trading risks and need suitable risk management tools. As a result, some carbon derivatives have been developed. At the moment futures and forwards on carbon emission allowances are fairly standard and are traded both over the counter (OTC) and on exchanges. Moreover, in October of 2006, European-style call and put options on EUA futures started trading in the European Climate Exchange (ECX). In

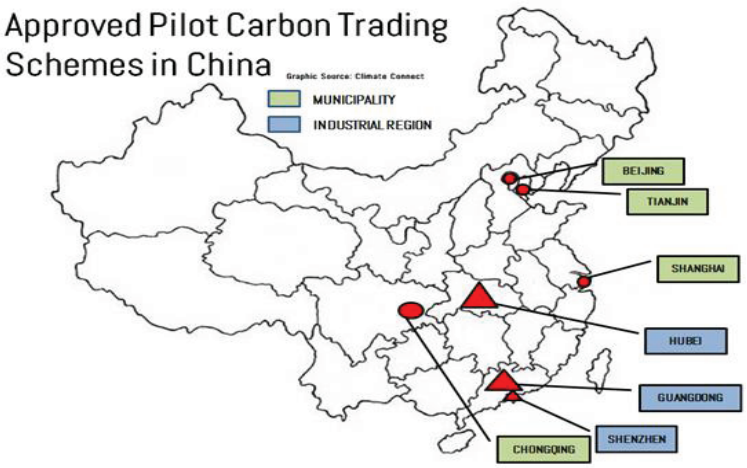


Figure 1: The mandatory emissions trading cities/regions in China (The source is from P. R. Shukla's report on "Emissions Cap and Trade: Implemen1tation Issues, Lessons and Recommendations").

https://doi.org/10.4208/aamm.2015.m1001 Published online by Cambridge University Press

order to hedge risks, a crucial problem is to capture the behaviour of carbon spot and futures prices and investigate the valuation and hedge of carbon derivatives.

Obviously, the problem of pricing CO_2-derivatives is important in theory and practice, and there are some works available on this problem. For the sake of completeness, we now briefly review the recent literature on the relation between spot and futures prices of EUAs. The paper [23] deals with risk-neutral allowance price formation within EU ETS in terms of marginal abatement costs and optimal stochastic control using equilibrium properties. Also, it has been showed that within the trading scheme the marginal costs of abatement are equal for each company, and the discounted marginal costs of abatement must be constant over time [19]. From a statistical point of view, the models proposed in [11] demonstrate that the non-mean reverting models perform better than the mean reverting ones in the EUA market and indeed confirm that a cost-of-carry model with the zero convenience yield leads to significant pricing errors for inter-phase futures contracts. However, they choose data from the first period to make the above analysis, where the market is neither as liquid as the second period, nor do market participants have sufficient experience with the underlying.

The valuation of option on emission allowances is addressed in [9], which considers the endogenous emission permit price dynamics within an equilibrium setting to value European options on emission allowances. On this topic, it is also worth highlighting that [11] discusses the empirical evidence from existing markets and develops an empirically and theoretically valid framework for the pricing and hedging of the intra-phase and the inter-phase futures and options on futures, respectively. In addition, the pricing equation has been derived and its numerical method has been developed in [21], which, however, cares only about different hedging strategies to account for jump risk and transaction costs. At the end of the first period, how to model the properties of CO_2 spot returns is shown in [17] which treats econometric aspects of emission allowance prices from the statistical distribution and their forecastability.

Generally, it is quite natural that the dynamics evolution of the emission price in the economic activities is introduced directly. A stochastic process is proposed to capture the behaviour of the unique equilibrium spot price, and the dynamics of carbon futures is derived under risk neutral by using a no-arbitrage principle in [10]. Moreover, [8] makes a rigorous analysis on a simple risk-neutral reduced-form model for allowance futures prices, demonstrates its calibration to historical data, and shows how to price European call options written on these contracts. The short-term spot price behavior and characteristic properties for financial time series are observed for prices of emission allowances from the new EU-wide CO_2 emissions trading system (EU ETS) in [5].

The classical log-normal diffusion model [7] cannot handle the "rare events", which have to do with the discontinuity of the observed price processes. There are several empirical researches supporting the presence of jumps especially in the interest rates, foreign exchange rates, and energy commodity price (see [11, 21]), and the jump model might explain the reason for the mispricing with respect to the Black-Scholes model [4]. In addition, different financial problems under jump diffusion processes are discussed

https://doi.org/10.4208/aamm.2015.m1001 Published online by Cambridge University Press

in [1–3]. Also, it is important to know how jumps might influence option valuations and investment decisions. Especially, in the presence of jump processes, the derivation of formulas for the valuations of derivatives is complicated by several factors [11].

To the best of the authors' knowledge, option pricing within EU ETS is considered only recently. Hence, the literature on the valuation of CO_2-derivatives is still sparse. The main contribution of this paper is to develop the model to price European option on CO_2 emissions allowance futures under the Merton's and the Kou's jump diffusions (see, for example, [18] and [22]). It is crucial to provide some intuition to understand for numerical method support by comparing with other results using different method. In fact, using the risk minimizing trading strategy, we obtain the pricing model governed by a partial differential equation (PDE). What is more, a so-called fitted finite volume method is provided to solve the mathematical model numerically. As we all know, although some option pricing models have exact solutions in terms of infinite series of special functions, in general it is more efficient to solve these numerically from a partial differential equation formulation rather than to approximate the infinite series. Especially, computers are very popular now, such that numerical methods are welcome for the computations of option valuations. For a market participant, it will be important to provide a quantitative framework for pricing emission derivatives by using an appropriate numerical method rather than a closed form solution. Also, it is crucial to provide some comparisons among some different numerical methods.

The reminder of the paper is organized as follows. Section 2 presents the necessary frameworks, makes assumptions, and derives the pricing partial differential equation based on the CO_2 emissions allowance in the EU ETS market, including the case in which the underlying asset price follows a jump-diffusion process. Then, under the risk-neutral measure and the jump-diffusion processes with various distributions of jump sizes, we obtain the pricing formulas of the European options. The mathematical treatment in Section 3 is primarily concerned with the approximation of the integral term arising from the pricing equation by the fast Fourier transform (FFT) method. The fitted finite volume method is presented in Section 4, where the fully discrete scheme is provided. We then proceed to give some numerical examples to confirm the theoretical results and the efficiency of the numerical method for the valuation of European options with different parameters in Section 5. Finally, Section 6 concludes this paper with some comments and gives future research.

2 Futures stochastic process and option valuation

2.1 Futures stochastic process

In order to price options on futures, first we need to obtain the stochastic process followed by the prices of futures. Next we will use Itô's lemma for jump processes in [20] and the risk-neutralized processes for spot price to gain the risk-neutralized process for futures price.

https://doi.org/10.4208/aamm.2015.m1001 Published online by Cambridge University Press

In view of the arriving of some information which may arouse the CO_2 allowance price to crash, or economical crisis and so on in the CO_2 derivatives market, we consider the emergence of jump factor in the spot price stochastic process. Furthermore, under the historical probability measure $\mathbb{P}$, the spot price stochastic differential equation can be described as follows:

$$dS_t=\mu(S_t,t)dt+\sigma(S_t,t)dW_t+J(S_t,t)dq_t, \tag{2.1}$$

where S_t is the EUA spot price at time t, W_t is a standard Wiener process, $\mu(S_t,t)$ is the drift, $\sigma(S_t,t)$ is the diffusion coefficient, and $J(S_t,t)$ is the jump amplitude. The drift, the diffusion, and the jump coefficients are assumed to be general functions of time and the EUA spot price. The jump component is controlled by a Poisson process q_t with constant arrival parameter λ, i.e., Prob $(dq_t=1)=\lambda dt$ and Prob $(dq_t=0)=1-\lambda dt$. In addition, dW_t, dq_t, and y are assumed to be mutually independent. For instance, we have the following concrete model of (2.1) (see [11]) given by

$$dS_t=(\mu-\lambda k)S_tdt+\sigma S_tdW_t+(y-1)S_tdq_t, \tag{2.2}$$

where dW_t is an increment of the standard Gauss-Wiener process, μ the drift rate, σ the volatility, y the jump size, and λ the average number of jumps per year, $k=E(y-1)$, and E is the expectation operator. Especially, in (2.2) y can be chosen to follow the log-normal density with μ and σ_j being the mean and the variance, respectively,

$$g(y)=\frac{1}{\sqrt{2\pi}\sigma_j y}\exp\Big(\frac{(\log(y)-\mu)^2}{2\sigma_j^2}\Big) \tag{2.3}$$

and $k=\exp(\mu+\sigma_j^2/2)-1$.

For the jump diffusion in (2.2), under the risk neutral measure $\mathbb{Q}$ its equivalent process is given as follows:

$$dS_t=(r-\delta-\lambda^*k^*)S_tdt+\sigma S_tdW_t+(y^*-1)S_tdq_t^*, \tag{2.4}$$

where δ is the current marginal net rate of convenience yield, and under the measure $\mathbb{Q}$, y^*, λ^*, and k^* have the same meanings as those in (2.2).

From [6] we know that the futures price F_t^T at time t with the expiration date T can be obtained as follows:

$$F_t^T=S_te^{(r-\delta)(T-t)}, \tag{2.5}$$

which is called the well-known one-factor cost-of-carry formula.

Jump diffusion process is used further in order to develop a framework for pricing both intra-phase and inter-phase options on futures. With a convenience yield δ, spot and futures prices are related through (2.5). However, it can be argued that for the intra-phase futures δ equals zero since storing permits within a certain period is costless and EUAs are required only once per year for compliance. Hence, there should not be any

https://doi.org/10.4208/aamm.2015.m1001 Published online by Cambridge University Press

advantage of holding a long futures position in comparison to holding a long spot position, that is, the convenience yield should be zero. Also, this can be explained through the cost-of-carry model, which states that if we assume a constant interest rate r and there are no storage costs or dividends, the only costs of holding the underlying is the foregone interest. Hence, the futures price $F_t(S_t,T)$ at time t for a contract on S_t maturing at time T is given by the standard cost-of-carry relationship:

$$F_t^T = S_t e^{r(T-t)}. \tag{2.6}$$

Using Itô's lemma for jump-diffusion processes, the dynamics of the futures price (2.6) can be represented as

$$dF = \left[F_t + \frac{1}{2}F_{ss}\sigma_s^2 S^2 + F_s(r-\lambda^* k^*)S\right]dt + F_s\sigma_s S dW_t + F_s S y^* dq_t^* \tag{2.7}$$

in differential notation under the risk-neutral measure.

According to [14] and (2.4), substituting F_t, F_s, F_{ss} into (2.7), we can obtain the futures price stochastic process as follows:

$$dF = -\lambda^* k^* F dt + \sigma_s F dW_t + F(y^*-1)dq_t^*. \tag{2.8}$$

2.2 The valuation of option on futures

Let $V(F,t)$ denote the value of a European contingent claim with striking price K on the underlying asset F and time t. According to (2.8), using standard arguments (see [25]), it is easy to show that $V(F,t)$ satisfies the following backward partial integro-differential equation (PIDE):

$$\frac{\partial V}{\partial t} + \frac{1}{2}\sigma^2 F^2 \frac{\partial^2 V}{\partial F^2} - \lambda^* k^* F \frac{\partial V}{\partial F} - rV + \lambda^* E(V(Fy^*,t) - V(F,t)) = 0, \tag{2.9}$$

with the final condition

$$V(F,T) = \max(K-F,0), \tag{2.10}$$

where $E(\cdot)$ is an expectation operator given by

$$E(V(Fy^*,t)) = \int_{-\infty}^{\infty} V(Fy^*)g(y^*)dy^*. \tag{2.11}$$

In Merton's model [16], $g(\cdot)$ is given by the log-normal density (2.3); in Kou's model [15], the log jump size is a distribution with the double exponential density, in other words, $g(\cdot)$ is given by the log-double-exponential probability density function:

$$g(y) = p\xi_1 \exp(-\xi_1 y)\mathcal{H}(y) + q\xi_2 \exp(\xi_2 y)\mathcal{H}(-y), \tag{2.12}$$

https://doi.org/10.4208/aamm.2015.m1001 Published online by Cambridge University Press

where $p,q>0$, $\xi_1>1$, $\xi_2>0$, $p+q=1$, $k^*=E(y^*-1)=\frac{p\xi_1}{\xi_1-1}+\frac{q\xi_2}{\xi_2-1}-1$ and $\mathcal{H}(y)$ is the Heaviside function.

As mentioned before, although some option pricing models have exact solutions in terms of infinite series, we would rather use numerical methods to solve them from a partial differential equation formulation than approximate the infinite series. To this purpose, we need to add artificial boundary conditions for the above problem (2.9). In fact, for a European put option on futures, by virtue of its financial meanings, the boundary conditions can be given by

$$V(0,t)=K\exp^{-r(T-t)}, \qquad t\in[0,T), \tag{2.13a}$$

$$V(F_{\max},t)=0, \qquad t\in[0,T), \tag{2.13b}$$

where $F_{\max}$ is a big number.

At present, we pay our attention to the relatively simple case of finite-activity compound Poisson jump diffusion process for a single underlying stochastic variable under Merton's model and Kou's model, deferring the treatment of the more complicated cases of general Levy processes and multiple state variables to future work. As in [24], we do not assume constant coefficients for the diffusion part of the process. Note that we have recently become aware of a paper in [26] which is similar in spirit to the methods suggested in this work, although the details of the implementation are different.

3 Jump integral discretization

In the section, we explore discretization methods for the integral or jump term in PIDE (2.9). The FFT evaluation of the integral will turn the expression (2.11) into a correlation product below. In fact, if let $x=\log F$ and $z=\log y^*$, then we have the following correlation product:

$$I=\int_{-\infty}^{\infty}\overline{V}(x+z)f(z)dz, \tag{3.1}$$

where $f(z)=g(e^z)e^z$ is the probability density of a jump of size $z=\log(y^*)$, and $\overline{V}(z)=V(\mathrm{e}^z)$. In particular, the discrete form of the correlation integral (3.1) requires an equally spaced grid in $\log F$ coordinates. However, a typical grid for the discretization of the PDE part in (2.9) will be unequally spaced in F coordinates. Therefore, as mentioned in [12], it is highly unlikely that two grids are fully compatible. Hence, we employ the linear interpolation between the two grids to determine the appropriate values.

In the following discussions, we will drop the superscript $*$ in the parameters to simplify the notation. In fact, all the processes and parameters below are under the risk neutral probability measure $\mathbb{Q}$.

Conveniently, we can write the correlation integral (3.1) in discrete form at an equally

https://doi.org/10.4208/aamm.2015.m1001 Published online by Cambridge University Press

spaced grid nodal point as

$$\bar{Q}(x_i) \simeq \bar{Q}_i = \sum_{j=-N/2+1}^{N/2} \overline{V}_{i+j} f_j \Delta z + \mathcal{O}((\Delta z)^2), \tag{3.2}$$

where $\overline{V}_k$ denotes the nodal approximation of $\overline{V}(k\Delta x)$ for any k, N a positive integer in the above, and

$$f_j = \frac{1}{\Delta z} \int_{z_j - \Delta z/2}^{z_j + \Delta z/2} f(z) dz. \tag{3.3}$$

When N is selected sufficiently large so that the solution in the areas of interest is not affected by the application of an asymptotic boundary condition for the large value of F. In particular, we assume that $V_{N/2+j}$ $(j>0)$ can be approximated by an asymptotic boundary condition. In practice, since f_j decays rapidly for $|j|>0$, this should not cause any difficulty. In addition, notice that $V_{-N/2+j}$ $(j<0)$ can be interpolated from the known values V_k, since these points represent values near $F=0$. In other words, since $f(z)$ decays exponentially as $|z|$ goes to infinity, we expect that $f(\pm N/2\Delta z) \simeq 0$. An important property to note is

$$f_j \geq 0, \quad \forall j \quad \text{and} \quad \sum_{j=-N/2+1}^{N/2} f_j \Delta z \leq 1. \tag{3.4}$$

This follows the fact that $f(y)$ is a probability density function and f_j is defined by Eq. (3.3). The discrete form of the correlation integral (3.2) uses an equally spaced grid in $\log F$ coordinates.

Assuming that f is real from a safe assumption for financial applications, the discrete correlation of Eq. (3.2) can be evaluated using the FFT by

$$\bar{Q}_i = IFFT(FFT(\overline{V}) \cdot (FFT(f))^*), \tag{3.5}$$

where IFFT stands for the inverse of the FFT and $(\cdot)^*$ denotes the complex conjugate. $FFT(f)$ can be pre-computed and stored for efficiency, since an FFT and an inverse of FFT must be computed during each time step.

Now we summarize the steps needed to generate the required values Q_i as follows.

First of all, in order to obtain approximation of $\bar{V}$, we use linear interpolation of the discrete values V on an equally spaced x grid. If $F_{\gamma(j)} \leq e^{j\Delta x} \leq F_{\gamma(j)+1}$, where $\gamma(j)$ is an index depending on j, then this generates the required values of $\overline{V}_j$:

$$\bar{V}_j = \psi_{\gamma(j)} V_{\gamma(j)} + (1-\psi_{\gamma(j)}) V_{\gamma(j)+1} + \mathcal{O}((\Delta F_{\gamma(j)})^2), \tag{3.6}$$

where $\psi_{\gamma(j)}$ is the interpolation weight, and $\Delta F_i = F_{i+1} - F_i$ for any integer.

Similarly, for any integer i, we assume that $q(i)$ is an index such that $e^{x_{q(i)}} \leq F_i \leq e^{x_{q(i)+1}}$. Then, we can define the approximation to $Q(F_i)$ given by

$$Q(F_i) = \phi_{q(i)} \bar{Q}(x_{q(i)}) + (1-\phi_{q(i)}) \bar{Q}(x_{q(i)+1}) + \mathcal{O}((\Delta e^{x_{q(i)}})^2), \tag{3.7}$$

https://doi.org/10.4208/aamm.2015.m1001 Published online by Cambridge University Press

where $\phi_{q(i)}$ is the interpolation weight. It is clear that

$$0\leq\psi_i\leq 1,\quad 0\leq\phi_i\leq 1. \tag{3.8}$$

Finally, combining (3.6) and (3.7) with (3.2), we obtain an approximation of $Q(F_i)$ given by

$$Q(F_i)=\sum_{j=-N/2+1}^{N/2}\Pi_j^i(V)f_j\Delta z+\mathcal{O}((\Delta z)^2), \tag{3.9}$$

where

$$\begin{aligned}\Pi_j^i(V)=&\phi_{q(i)}\left[\psi_{\gamma(q(i)+j)}V_{\gamma(q(i)+j)}+(1-\psi_{\gamma(q(i)+j)})V(F_{\gamma(q(i)+j)+1})\right]\\&+(1-\phi_{q(i)})\left[\psi_{\gamma(q(i)+j+1)}V(F_{\gamma(q(i)+j+1)})\right.\\&\left.+(1-\psi_{\gamma(q(i)+j+1)})V(F_{\gamma(q(i)+1+j)+1})\right].\end{aligned} \tag{3.10}$$

Algorithm 3.1. The method for computing the integral term in Eq. (3.1) by the FFT can be represented as:

1. Interpolate the discrete values of V on an equally spaced $\log F$ grid, which can generate the required values of V_j.
2. Carry out the FFT on the $\overline{V}$ data. Compute the correlation in the frequency domain (with pre-computed $FFT(f)$ values), using (3.5).
3. Invert the FFT of the correlation.
4. Interpolate the discrete values of Q_i back on the original F grid.

In addition, the matrix R arising from discretization of correlation product term is dense, and applying the FFT approach to $R\widehat{V}^l$ will produce undesirable wrap-around pollution. Therefore, in order to reduce the effect of FFT wrap-around, a commonly used technique is to embed the Toeplitz matrix R into the circulant matrix C as the product of a circulant matrix times a vector, where

$$R=\begin{bmatrix} f_0 & f_1 & f_2 & \cdots & f_N\\ f_{-1} & f_0 & f_1 & \cdots & f_{N-1}\\ f_{-2} & f_{-1} & f_0 & \cdots & f_{N-2}\\ \vdots & \vdots & \ddots & \cdots & \vdots\\ \vdots & \vdots & \vdots & \ddots & \vdots\\ f_{-N} & f_{1-N} & f_{2-N} & \cdots & f_0 \end{bmatrix} \tag{3.11}$$

https://doi.org/10.4208/aamm.2015.m1001 Published online by Cambridge University Press

and

$$C=\begin{bmatrix} f_0 & f_1 & f_2 & \cdots & f_N & f_{-N} & f_{1-N} & f_{2-N} & \cdots & f_0 \\ f_{-1} & f_0 & f_1 & \cdots & f_{N-1} & f_N & f_{-N} & f_{1-N} & \cdots & f_{N-1} \\ f_{-2} & f_{-1} & f_0 & \cdots & f_{N-2} & f_{N-1} & f_N & f_{-N} & \cdots & f_{N-2} \\ \vdots & \vdots & \vdots & \cdots & \vdots & \vdots & \vdots & \vdots & \cdots & \vdots \\ \vdots & \vdots & \vdots & \cdots & \vdots & \vdots & \vdots & \vdots & \cdots & \vdots \\ f_{-N} & f_{1-N} & f_{2-N} & \cdots & f_0 & f_1 & f_2 & f_3 & \cdots & f_N \\ f_N & f_{-N} & f_{1-N} & \cdots & f_{-1} & f_0 & f_1 & f_2 & \cdots & f_{N-1} \\ f_{N-1} & f_N & f_{-N} & \cdots & f_{-2} & f_{-1} & f_0 & f_1 & \cdots & f_{N-2} \\ f_{N-2} & f_{N-1} & f_N & \cdots & f_{-3} & f_{-2} & f_{-1} & f_0 & \cdots & f_{N-3} \\ \vdots & \vdots & \vdots & \cdots & \vdots & \vdots & \vdots & \vdots & \cdots & \vdots \\ \vdots & \vdots & \vdots & \cdots & \vdots & \vdots & \vdots & \vdots & \cdots & \vdots \\ f_1 & f_2 & f_3 & \cdots & f_{-N} & f_{1-N} & f_{2-N} & f_{3-N} & \cdots & f_0 \end{bmatrix}. \tag{3.12}$$

Each row in the above circulant matrix is by definition a circular shift of the previous row, a property that reflects the periodicity of the sequence in the convolution.

4 The fitted finite volume method

In this section, on the basis of the work in [24], we construct a fitted finite volume method for (2.9). To this purpose, we first rewrite the problem (2.9) as the following divergent form:

$$-\frac{\partial V}{\partial t}-\frac{\partial}{\partial F}\left(aF^2\frac{\partial V}{\partial F}+bFV\right)+cV-\lambda Q(F)=0, \tag{4.1}$$

where

$$a=\frac{1}{2}\sigma^2,\quad b=-\lambda k-\sigma^2,\quad c=r+\lambda+b=r-\sigma^2-\lambda(k-1).$$

Let the interval $I=(0,F_{\max})$ be divided into N sub-intervals:

$$I_i:=(F_i,F_{i+1}),\quad i=0,1,\cdots,N-1,$$

with $0=F_0<F_1<\cdots<F_N=F_{\max}$. For each $i=0,1,\cdots,N-1$, we put $h_i=F_{i+1}-F_i$ and $h=\max_{0\le i\le N-1}h_i$. We also let $F_{i-1/2}\in(F_{i-1},F_i)$ and $F_{i+1/2}\in(F_i,F_{i+1})$ be two mid-points for each $i=1,2,\cdots,N-1$. These points form a second partition of $(0,F_{\max})$ if we define $F_{-1/2}=F_0$ and $F_{N+1/2}=F_N$. Integrating both sides of (4.1) over $(F_{i-1/2},F_{i+1/2})$, we have

$$-\int_{F_{i-1/2}}^{F_{i+1/2}}\frac{\partial V}{\partial t}dF-\left[F\left(aF\frac{\partial V}{\partial F}+bV\right)\right]_{F_{i-1/2}}^{F_{i+1/2}}+\int_{F_{i-1/2}}^{F_{i+1/2}}cVdF-\lambda\int_{F_{i-1/2}}^{F_{i+1/2}}Q(F)dF=0, \tag{4.2}$$

for $i=1,2,\cdots,N-1$. Applying the one-point quadrature rule to the first, third and last terms, we obtain from the above

$$-\frac{\partial V_i}{\partial t}l_i-\left[F_{i+1/2}\rho(V)|_{F_{i+1/2}}-F_{i-1/2}\rho(V)|_{F_{i-1/2}}\right]+c_iV_il_i-\lambda Q_il_i=0, \tag{4.3}$$

https://doi.org/10.4208/aamm.2015.m1001 Published online by Cambridge University Press

for $i=1,2,\cdots,N-1$, where $l_i=F_{i+1/2}-F_{i-1/2}$, $c_i=c(F_i,t)$, $Q_i=Q(F_i,t)$, V_i is the nodal approximation to $V(F_i,t)$ to be determined, and $\rho(V)$ is a flux associated with V defined by

$$\rho(V):=aF\frac{\partial V}{\partial F}+bV. \tag{4.4}$$

We now need to find an approximation to $\rho(V)$ defined above at the mid-point $F_{i+1/2}$ of the interval I_i for all $i=0,1,\cdots,N-1$. This discussion is divided into two cases that $i\geq 1$ and $i=0$, respectively.

Case I. Approximation of ρ at $F_{i+1/2}$ for $i\geq 1$. Let us consider the following two-point boundary value problem:

$$(aFv'+b_{i+1/2}v)'=0, \qquad F\in I_i, \tag{4.5a}$$
$$v(F_i)=V_i, \qquad v(F_{i+1})=V_{i+1}, \tag{4.5b}$$

where $b_{i+1/2}=b(x_{i+1/2},t)$. Integrating (4.5a) yields the first order linear equation

$$\rho_i(v):=aFv'+b_{i+1/2}v=C_1,$$

where C_1 denotes an additive constant. Solving this linear system gives

$$\rho_i(v)=C_1=b_{i+1/2}\frac{F_{i+1}^{\eta_i}V_{i+1}-F_i^{\eta_i}V_i}{F_{i+1}^{\eta_i}-F_i^{\eta_i}}, \tag{4.6}$$

where $\eta_i=b_{i+1/2}/a$.

Case II. Approximation of ρ at $F_{1/2}$. Similarly, we can analyze the approximation of the flux at $F_{1/2}$. Note that the analysis in Case I cannot be applied to the approximation of the flux on $I_1=(0,F_1)$ because (4.5a) is degenerate. To smooth away this difficulty, we consider another ordinary differential equation with an extra degree of freedom in the following form:

$$aFv'+b_{i+1/2}v=C, \qquad F\in I_1, \tag{4.7a}$$
$$v(F_0)=V_0, \qquad v(F_1)=V_1. \tag{4.7b}$$

Solving this problem analytically gives

$$\rho_1(v)=(aFv'+b_{1/2}v)_{F_{1/2}}=\frac{1}{2}[(a+b)V_1-(a-b)V_0], \tag{4.8a}$$
$$V=V_0+(V_1-V_0)F/F_1, \quad F\in I_1=(0,F_1). \tag{4.8b}$$

Thus, it follows from substituting (4.6) or (4.8), depending on the value of i, and (3.9) into (4.3) that for $\tau=T-t$

$$\frac{\partial V_i}{\partial\tau}=\alpha_iV_{i-1}+\beta_iV_i+\gamma_iV_{i+1}+\lambda\sum_{j=-N/2+1}^{N/2}\Pi_j^i(V)f_j\Delta y, \tag{4.9}$$

https://doi.org/10.4208/aamm.2015.m1001 Published online by Cambridge University Press

where

$$\alpha_1=\frac{F_1}{4l_1}(a-b_{1/2}),\qquad \beta_1=\frac{b_{1+1/2}F_{1+1/2}F_2^{\eta_1}}{l_1(F_2^{\eta_1}-F_1^{\eta_1})},$$
$$\gamma_1=-\frac{F_1}{4l_1}(a+b_{1+1/2})-\frac{b_{1+1/2}F_{1+1/2}F_1^{\eta_1}}{l_1(F_2^{\eta_1}-F_1^{\eta_1})}-c_1,$$
$$\alpha_i=\frac{b_{i-1/2}F_{i-1/2}F_{i-1}^{\eta_{i-1}}}{(F_i^{\eta_{i-1}}-F_{i-1}^{\eta_{i-1}})l_i},\qquad \beta_i=\frac{b_{i+1/2}F_{i+1/2}F_{i+1}^{\eta_i}}{l_i(F_{i+1}^{\eta_i}-F_i^{\eta_i})},$$
$$\gamma_i=-\frac{b_{i-1/2}F_{i-1/2}F_i^{\eta_{i-1}}}{(F_i^{\eta_{i-1}}-F_{i-1}^{\eta_{i-1}})l_i}-\frac{b_{i+1/2}F_{i+1/2}F_i^{\eta_i}}{l_i(F_{i+1}^{\eta_i}-F_i^{\eta_i})}-c_i,$$

for $i=2,\cdots,N$.

Next we discuss the time discretization of the linear ordinary differential equation system (4.9). Therefore, insert N_t-1 points in $[0,T]$: $T=t_0>t_1>\cdots>t_{N_t}=0$, and choose the two-level implicit time-stepping method with a splitting parameter $\theta=1/2$, or Crank-Nicolson scheme, to ensure that the time-stepping scheme is of 2nd-order accuracy. Thus, the full Crank-Nicolson scheme is as follows:

$$V_i^{n+1}\left[1-\frac{\Delta\tau_n\gamma_i}{2}\right]-\frac{\Delta\tau_n\alpha_i}{2}V_{i-1}^{n+1}-\frac{\Delta\tau_n\beta_i}{2}V_{i+1}^{n+1}-\lambda\frac{\Delta\tau_n}{2}\sum_{j=-N/2+1}^{N/2}\Pi_j^i(V^{n+1})f_j\Delta y$$
$$=V_i^n\left[1+\frac{\Delta\tau_n\gamma_i}{2}\right]+\frac{\Delta\tau_k\alpha_i}{2}V_{i-1}^n+\frac{\Delta\tau_n\beta_i}{2}V_{i+1}^n+\lambda\frac{\Delta\tau_n}{2}\sum_{j=-N/2+1}^{N/2}\Pi_j^i(V^n)f_j\Delta y,\qquad(4.10)$$

for $n=0,\cdots,N_t$, where V_i^n denotes the nodal approximation to $V(F_i,\tau_n)$, $\Delta\tau_n=t_n-t_{n-1}$. Note that the above expressions are invalid for $i=0,N$ because of the Dirichlet boundary conditions at the two points. To incorporate these boundary nodes in the second and Nth equations in (4.10), we replace V_0^{n+1} and V_N^{n+1} in the two equations with the corresponding Dirichlet boundary conditions in (2.13). Denoting the vector $V^n=[V_0^n,\cdots,V_N^n]$ and $N\times N$ matrices M and $D=(d_{ij})$, such that

$$[MV^n]_i=-\frac{\Delta\tau_n\alpha_i}{2}V_{i-1}^n-\frac{\Delta\tau_n\gamma_i}{2}V_i^n-\frac{\Delta\tau_n\beta_i}{2}V_{i+1}^n,\qquad(4.11a)$$
$$[DV^n]_i=-\lambda\frac{\Delta\tau_n}{2}\sum_{j=-N/2+1}^{N/2}d_{ij}V_i=-\lambda\frac{\Delta\tau_n}{2}\sum_{j=-N/2+1}^{N/2}\Pi_j^i(V^n)f_j\Delta y,\qquad(4.11b)$$

we get the following matrix form of (4.10):

$$[I+M+D]V^{n+1}=[I-M-D]V^n,\qquad(4.12)$$

where I is the identity matrix.

https://doi.org/10.4208/aamm.2015.m1001 Published online by Cambridge University Press

When using an implicit discretization to solve the system (4.12), it is computationally inefficient to solve it because the correlation product term makes the system matrix dense. Thus, in this section we will explore the use of iteration to solve the linear system (4.12). First of all, we have the following stability result.

Theorem 4.1 (Stability of scheme (4.10))**.** *The discretization scheme* (4.10) *is unconditionally stable for the given θ provided that*

(1) $\alpha_i,\beta_i\geq 0$;

(2) the discrete probability density f_j *has the properties* (3.4);

(3) the interpolation weights satisfy (3.8);

(4) $r,\lambda\geq 0$.

Proof. Let $V^n=[V_0^n,V_1^n,V_2^n,\cdots,V_N^n]^\top$ be the solution vector to (4.10). For any $n=0,2,\cdots,N_t$, we suppose that the initial solution vector is perturbed, i.e., $\hat{V}^0=V^0+E^0$, and $E^n=[E_0^n,\cdots,E_N^n]^\top$ denote the perturbation vector in the nth time step with $E_0^n=E_N^n=0$ due to the Dirichlet boundary conditions. From (4.10) we have

$$\begin{aligned}&E_i^{n+1}\left[1-\frac{\Delta\tau_n\gamma_i}{2}\right]-\frac{\Delta\tau_n\alpha_i}{2}E_{i-1}^{n+1}-\frac{\Delta\tau_n\beta_i}{2}E_{i+1}^{n+1}-\lambda\frac{\Delta\tau_n}{2}\sum_{j=-N/2+1}^{N/2}\Pi_j^i(E^{n+1})f_j\Delta y\\&=E_i^n\left[1+\frac{\Delta\tau_n\gamma_i}{2}\right]+\frac{\Delta\tau_n\alpha_i}{2}E_{i-1}^n+\frac{\Delta\tau_n\beta_i}{2}E_{i+1}^n+\lambda\frac{\Delta\tau_n}{2}\sum_{j=-N/2+1}^{N/2}\Pi_j^i(E^n)f_j\Delta y.\end{aligned}\tag{4.13}$$

Defining a discrete maximum norm by

$$\|E^n\|_\infty=\max_i|E_i^n|,\tag{4.14}$$

it follows from the above condition that

$$\begin{aligned}&|E_i^{n+1}|\left[1-\frac{\Delta\tau_n\gamma_i}{2}\right]\\&\leq\|E^n\|_\infty\left[1+\frac{\Delta\tau_n\gamma_i}{2}\right]+\frac{1}{2}\Delta\tau_n\lambda\|E^{n+1}\|_\infty+\frac{1}{2}\Delta\tau_n\lambda\|E^n\|_\infty\\&\quad+\frac{1}{2}\Delta\tau_n\alpha_i|E_{i-1}^{n+1}|+\frac{1}{2}\Delta\tau_n\beta_i|E_{i+1}^{n+1}|+\frac{1}{2}\Delta\tau_n\alpha_i|E_{i-1}^n|+\frac{1}{2}\Delta\tau_n\beta_i|E_{i+1}^n|.\end{aligned}\tag{4.15}$$

This implies

$$\begin{aligned}&|E_i^{n+1}|\left[1-\frac{\Delta\tau_n\gamma_i}{2}\right]\\&\leq\|E^n\|_\infty\left[1+\frac{\Delta\tau_n\gamma_i}{2}\right]+\frac{1}{2}\Delta\tau_n\lambda\|E^{n+1}\|_\infty+\frac{1}{2}\Delta\tau_n\lambda\|E^n\|_\infty+\frac{1}{2}\Delta\tau_n\alpha_i\|E^{n+1}\|_\infty\\&\quad+\frac{1}{2}\Delta\tau_n\beta_i\|E^{n+1}\|_\infty+\frac{1}{2}\Delta\tau_n\alpha_i\|E^n\|_\infty+\frac{1}{2}\Delta\tau_n\beta_i\|E^n\|_\infty,\end{aligned}\tag{4.16}$$

https://doi.org/10.4208/aamm.2015.m1001 Published online by Cambridge University Press

which is valid for all $i=0,1,\cdots,N$ and $n=0,1,\cdots,N_t$. In particular, it is true for node i^*, where

$$\max_i |E_i^{n+1}| = |E_{i^*}^{n+1}|. \tag{4.17}$$

Therefore, it follows from taking $i=i^*$ in (4.16) and Theorem 1 in [26]: $\lambda+\alpha_i+\beta_i+\gamma_i=-r$ that

$$\|E^{n+1}\|_\infty \Big[1+\frac{\Delta\tau_n r}{2}\Big] = \|E^n\|_\infty \Big[1-\frac{\Delta\tau_n r}{2}\Big],$$

and thus

$$\|E^{n+1}\|_\infty \le \|E^n\|_\infty \frac{1-\frac{\Delta\tau_n r}{2}}{1+\frac{\Delta\tau_n r}{2}} \le \cdots \le \Big(\frac{1-\frac{\Delta\tau_n r}{2}}{1+\frac{\Delta\tau_n r}{2}}\Big)^n \|E^0\|_\infty \le 1,$$

where

$$\lim_{n\to\infty}\Big(\frac{1-\frac{\Delta\tau_n r}{2}}{1+\frac{\Delta\tau_n r}{2}}\Big)^n = 0, \quad \text{since } \Big|\frac{1-\frac{\Delta\tau_n r}{2}}{1+\frac{\Delta\tau_n r}{2}}\Big| < 1.$$

Thus, we complete the proof. □

Remark 4.1. Obviously, it is easy to derive from the proof of Theorem 4.1 that

$$\|E^{n+1}\|_\infty \le \|E^n\|_\infty.$$

Also, we have the following convergence result.

Theorem 4.2 (Convergence of the iteration)**.** *Provided that*

(1) $\alpha_i, \beta_i \ge 0$;

(2) the discrete probability density f_j *has the properties* (3.4);

(3) the interpolation weights satisfy (3.8);

(4) $r>0$; $\lambda \ge 0$,

then the iteration of (4.12) *is globally convergent, and the maximum error at each iteration satisfies*

$$\|e^{k+1}\|_\infty \le \|e^k\|_\infty \frac{\frac{1}{2}\lambda\Delta\tau_k}{1+\frac{1}{2}(r+\lambda)\Delta\tau_k}.$$

Proof. As shown in Theorem 5.1 [13], we can easily get the proof of Theorem 4.2. □

Remark 4.2. According to Theorem 1 in [26], the matrix $I+M+D$ in (4.12) is an M-matrix when h and $\Delta\tau=\max_k\{\Delta\tau_k\}$ are sufficiently small.

https://doi.org/10.4208/aamm.2015.m1001 Published online by Cambridge University Press

5 Numerical experiments

In this section, some European option test problems with different parameters are presented to show the efficiency, usefulness, and convergence rate of the proposed discretization method. Also, the pictures of hedging parameters Δ and Γ are plotted. For each example, the number of grid points is doubled by dividing the time-step size ($\Delta\tau =$ 0.01 on the coarsest grid) into half. Moreover, the convergence ratio is defined as follows:

$$\text{Ratio } (\|\cdot\|_\infty) = \frac{\|V_{h/2}^{\Delta\tau/2} - V_h^{\Delta\tau}\|_\infty}{\|V_{h/4}^{\Delta\tau/4} - V_{h/2}^{\Delta\tau/2}\|_\infty}, \tag{5.1}$$

where V_α^β denotes the computed solution on the mesh with spatial mesh α and time mesh size β. In addition, the numerical order of convergence is then defined by

$$\text{Rate} = \log_2 \text{Ratio}.$$

Test 1. Here we employ our numerical method discussed in the above to compute the put option with the final condition and the boundary conditions (2.13) for the Merton's model. Moreover, the parameter values are used to value European vanilla put option under the log-normal jump diffusion process: σ=0.15, r=0.05, μ=−0.90, λ=0.10, T=0.25, $K = 100$, and $F_{\max} = 256$.

In the whole model, we choose $F_{\max} = 256$ to ensure the accuracy of the computed solution. In addition, the values of h are chosen to be multiples of 2, which is required by the FFT algorithm. With the above parameters, the numerical results for the put option are listed in Table 1.

From the above table we can see that our numerical scheme is convergent at the quadratic rate, since the Ratios approximate 4. The iteration method is under the tolerance 10^{-8}, which shows the fitted finite volume method combined with the Crank-Nicolson scheme is very efficient. Moreover, in order to compare the above results with these by the the closed form method and the Monte Carlo simulation method, we compute the option on future contract using the two algorithm to obtain the prices 3.6751

Table 1: The computed values of a European put option at $F = 100$ under Merton's jump model using the Crank-Nicolson time-stepping. The interpolation schemes are used to transfer data between the non-uniform F grids and the uniform log-spaced FFT grids.

x-step	t-step	Values at K	$\|V_{h/2}^{\Delta\tau/2} - V_h^{\Delta\tau}\|_\infty$	Ratio
64	25	3.452495194552296		
128	50	3.589205720268297	0.136710525716001	
256	100	3.619524797286868	0.030319077018571	4.5091
512	200	3.626942125909804	0.007417328622936	4.0876
1024	400	3.628787222958996	0.001845097049192	4.0200
2048	800	3.629247941271714	0.000460718312718	4.0048
4096	1600	3.629363085126250	0.000115143854536	4.0012

https://doi.org/10.4208/aamm.2015.m1001 Published online by Cambridge University Press

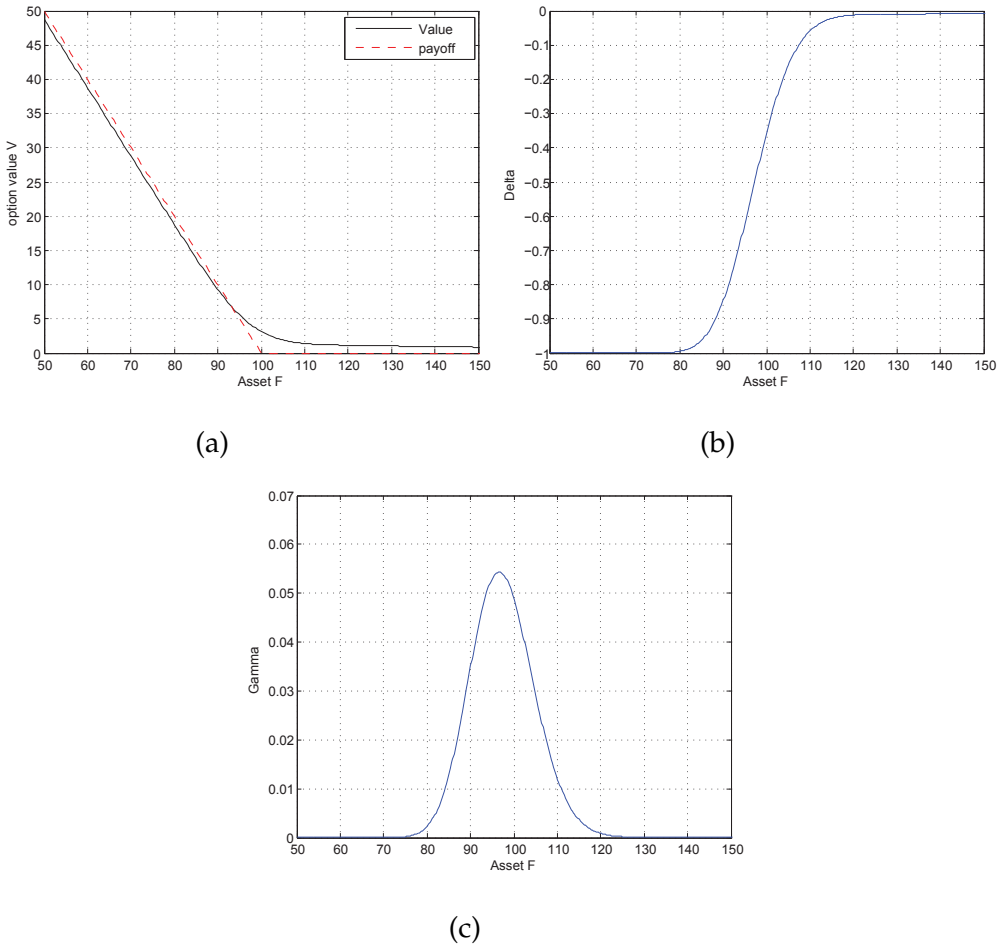


Figure 2: Put option value, Delta and Gamma for log-normal probability density function under Merton's jump diffusion model at $t=0$: (a) option value and payoff; (b) hedging parameter Delta V_F; (c) hedging parameter Gamma V_{FF}.

from the closed form and 3.6338 from the Monte Carlo simulation, respectively. This implies that the error between the closed form solution and the Monte Carlo method is 0.0413. However, the error between the closed form solution and the numerical method is 0.0457, which essentially means that the numerical result is quite acceptable and reasonable. In addition, the closed form pricing formula involves an infinite series, in which, generally speaking, the first 100 terms are needed to compute the option values.

Also, in Fig. 2 we plot the option values and its first and second derivatives (Greeks), Delta and Gamma, at $t=0$ for the European put vanilla option. Three figures show that the option values and Greeks are very stable and no spurious oscillations occur, which demonstrates that the fitted finite volume method combined with the Crank-Nicolson scheme is quite robust.

https://doi.org/10.4208/aamm.2015.m1001 Published online by Cambridge University Press

Test 2. Again we use our numerical method to compute the put option with final condition and boundary conditions (2.13) and under the Kou's jump model. Here the parameters, which are the same as those in [13], are chosen as follows: $r=0.05$, $\sigma=0.15$, $\xi_1=3.0465$, $\xi_2=3.0775$, $p=0.3445$, $\lambda=0.1$, $T=0.25$, $K=100$, and $F_{\max}=256$. The numerical results are listed in Table 2.

Table 2: The computed values of a European put option at $F=100$ under Kou's jump model using the Crank-Nicolson time-stepping. The interpolation schemes are used to transfer data between the non-uniform F grids and the uniform log-spaced FFT grids.

x-step	t-step	Values at K	$\|V_{h/2}^{\Delta\tau/2}-V_h^{\Delta\tau}\|_\infty$	Ratio
64	25	3.091542923		
128	50	3.178132626	0.086589703	
256	100	3.197478907	0.01934628	4.475780449
512	200	3.202233537	0.00475463	4.068935017
1024	400	3.203418524	0.001184987	4.012390519
2048	800	3.203714606	0.000296082	4.002218747
4096	1600	3.203788611	7.40045×10^{-5}	4.000871221

Once again, from the above table we can see that the convergent rate of our fitted finite volume method combined with the Crank-Nicolson numerical method is 2, and the iteration tolerance is under 10^{-8}. In [15], the closed form formula is given to solve option on futures contract price, and it is 3.22847 by the finite terms truncation. For the sake of comparison, the option price is computed by the Monte Carlo method, and it is 3.259742. In contrast, the fitted finite volume method is effective and feasible.

In addition, in Fig. 3 we plot the option value, its Delta and Gamma at $t=0$ for the European put vanilla option, from which we can see that no spurious oscillations occur.

6 Conclusions and further researches

In the most mature financial markets, a large volume of allowance futures is traded. European options written on these futures are introduced and traded, although no solid theoretical foundation for their valuations is available yet. On the basis of stochastic process for futures of CO_2 permits, this paper applies options pricing theory, taking CO_2 emission allowance futures as an underlying asset, to establish the mathematical model which reflects the value of options on CO_2 emission allowance futures with Merton's and Kou's jumps, respectively. Moreover, a so-called fitted finite element method combined with the fast Fourier transform and the Crank-Nicolson time stepping is proposed to solve the resulting option pricing model, and its stability and convergence are shown.

As mentioned before, the numerical method for the pricing model will be more viable, accurate to make the carbon emission decisions if the investment is needed. To some extent, quantitative analysis greatly reduces the error between theory and practice, and avoids the arbitrary individualism because of the lack of theoretical basis. We

https://doi.org/10.4208/aamm.2015.m1001 Published online by Cambridge University Press

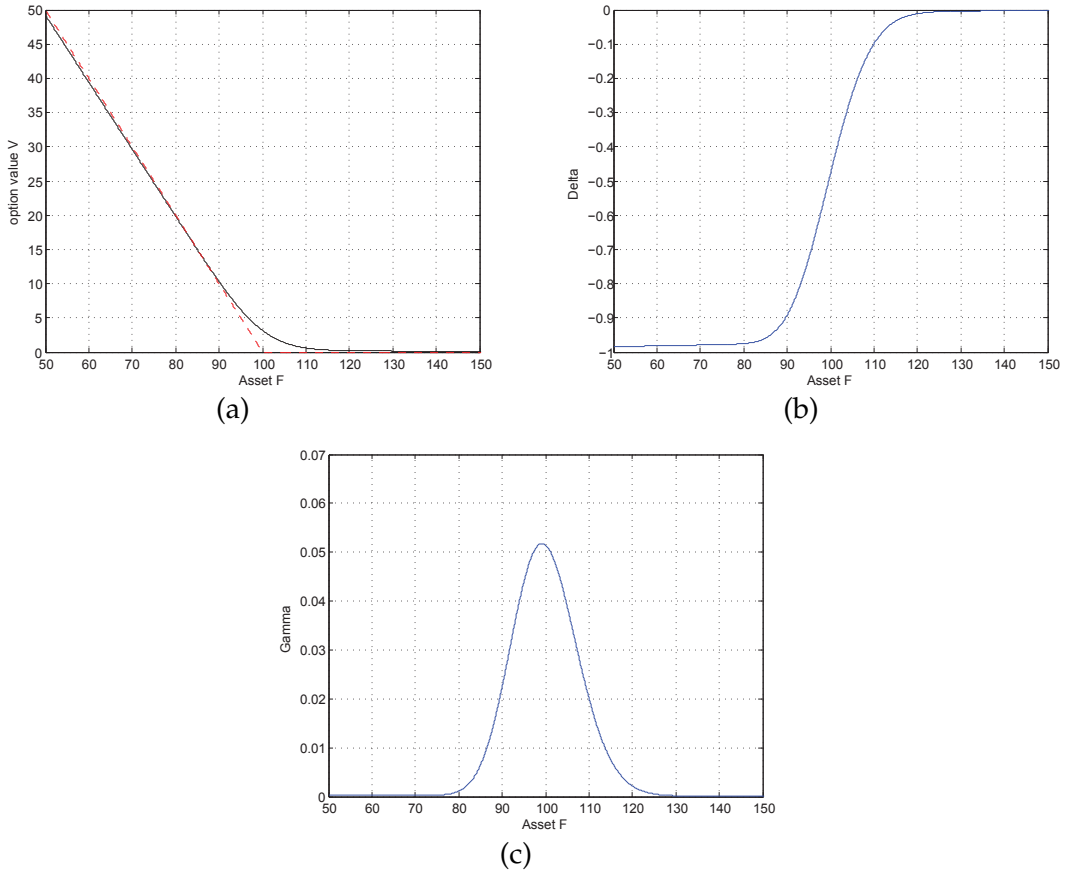


Figure 3: Put option value, Delta and Gamma for log-double-exponential probability density function under Kou's jump diffusion model at $t=0$: (a) option value and payoff; (b) hedging parameter Delta V_F; (c) hedging parameter Gamma V_{FF}.

hope that our findings are useful, and believe that quantitative modeling in the spirit of our approach can help regulatory authorities or managers to accurately make decisions. Also, the sensitivity parameters, Delta and Gamma, are presented. In addition, some numerical experiments are presented to demonstrate the efficiency and usefulness of this established numerical method.

Nevertheless, real-world carbon finance problems are much more complicated. Therefore, in the future works, we will consider the effects of stochastic convenience yields and stochastic interest rates on futures option pricing. Furthermore, the one-factor model is clearly inappropriate when there are abnormal conditions in the commodity market during the term of the contract, e.g., when the convenience yield is far above or far below its long-run mean. So, we will extend our study to the two-factor or three-factor models, considering the stochastic convenience yields or interest rates, which is close to the real situation.

https://doi.org/10.4208/aamm.2015.m1001 Published online by Cambridge University Press

Acknowledgments

The author would like to thank the referees for the helpful suggestions. This project was supported in part by the National Basic Research Program (No. 2012CB955804), the Major Research Plan of the National Natural Science Foundation of China (No. 91430108), the National Natural Science Foundation of China (No. 11171251), and the Major Program of Tianjin University of Finance and Economics (No. ZD1302).

References

[1] C. AHN, *Opion pricing when jump risk is systematic,* Math. Finance, 2 (1992), pp. 299–308.
[2] C. AHN AND H. THOMSON, *Jump-diffusion processes and the term structure of interest rates,* J. Finance, 43 (1988), pp. 155–174.
[3] K. AMIN, *Jump diffusion option valuation in discrete time,* J. Finance, 48 (1993), pp. 1863–1883.
[4] G. BAKSHI, C. CAO, AND Z. CHEN, *Empirical performance of alternative option pricing models,* J. Finance, 52 (1997), pp. 2003–2049.
[5] E. BENZ AND S. TRÜCK, *Modeling the price dynamics of CO_2 emission allowances,* Energy Economics, 31 (2009), pp. 4–15.
[6] F. BLACK, *The pricing of commodity contracts,* J. Financial Economics, 3 (1976), pp. 167–179.
[7] F. BLACK AND M. SCHOLES, *The pricing of options and corporate liabilities*, J. Political Economy, 81 (1973), pp. 637–659.
[8] R. CARMONA AND J. HINZ, *Risk-neutral models for emission allowance prices and option valuation,* Management Science, 57 (2011), pp. 1453–1468.
[9] M. CHESNEY AND L. TASCHINI, *The endogenous price dynamics of the emission allowances: An application to CO_2 option pricing,* Swiss Finance Institute Research Paper, Swiss Finance Institute, Zurich, 2008.
[10] C. CHURCH, Carbon Trading, Master Scinece Thesis, University of Oxford, 2009.
[11] G. DASKALAKIS, D. PSYCHOYIOS, AND R. N. MARKELLOS, *Modeling CO_2 emission allowance prices and derivatives: Evidence from the European trading scheme,* J. Bank. Finance, 33 (2009), pp. 1230–1241.
[12] Y. D'HALLUIN, P. A. FORSYTH, AND G. LABAHN, *A power penalty method for American options with jump diffusion processes,* Numerische Mathematik, 97 (2004), pp. 321–352.
[13] Y. D'HALLUIN, P. A. FORSYTH, AND K. R. VETZAL, *Robust numerical methods for contingent claims under jump-diffusion processes,* IMA J. Numer. Anal., 25 (2005), pp. 87–112.
[14] J. E. HILLIARD AND J. REIS, *Valuation of commodity futures and options under stochastic convenience yields, interest rates, and jump diffusion in the spot,* J. Financial Economics Quant. Anal., 33 (1998), pp. 61–86.
[15] S. G. KOU, *A jump-diffusion model for option pricing,* Management Sci., 48 (2002), pp. 1086–1101.
[16] R. C. MERTON, *Option pricing when underlying stock returns are discontinuous,* J. Financial Economics, 3 (1976), pp. 125–144.
[17] S. M. PAOLELLA AND L. TASCHINIA, *An econometric analysis of emission allowance prices,* J. Bank. Finance, 10(32) (2008), pp. 2022–2032.
[18] H. PHAM, *Optimal stopping, free boundary, and American option in a jump-diffusion model*, Appl. Math. Optim., 35 (1997), pp. 145–164.

https://doi.org/10.4208/aamm.2015.m1001 Published online by Cambridge University Press

[19] J. D. RUBIN, *A model of intertemporal emission trading, banking, and borrowing*, J. Environmental Economics Management, 31 (1996), pp. 269–286.
[20] S. E. SHREVE, Stochastic Calculus and Finance, Springer: New York, 2004.
[21] M. TILLMANN, Valuation and Hedging of Carbon-Derivatives, Institut für Numerische und Angewandte Mathematik Fachbereich Mathematik, 2008.
[22] J. TOIVANEN, *Numerical valuation of European and American options under Kou's jump-diffusion model*, SIAM J. Sci. Comput., 30 (2008), pp. 1949–1970.
[23] M. UHRIG-HOMBURG AND M. WAGNER, *Futures price dynamics of CO_2 emission certificates: an empirical analysis*, Working Paper, University of Karlsruhe, 2007.
[24] S. WANG, *A novel fitted finite volume method for the Black-Scholes equation governing option pricing*, IMA J. Numer. Anal., 24 (2004), pp. 699–720.
[25] P. WILMOTT, J. DEWYNNE, AND S. HOWISON, Option Pricing: Mathematical Models and Computation, Oxford Financial Press, Oxford, 1993.
[26] K. ZHANG AND S. WANG, *Pricing option under jump diffusion processes with fitted finite volume method*, J. Appl. Math. Comput., 201 (2008), pp. 398–413.
[27] K. ZHANG AND S. WANG, *A computational scheme for option under jump diffusion processes*, J. Appl. Math. Comput., 6 (2009), pp. 110–123.

https://doi.org/10.4208/aamm.2015.m1001 Published online by Cambridge University Press